UNIVERSITY OF BIRMINGHAM

University of Birmingham Research at Birmingham

Randomness and frustration in a S=½ square-lattice Heisenberg antiferromagnet

Fogh, Ellen; Mustonen, Otto; Babkevich, Peter; Katukuri, Vamshi M.; Walker, Helen C.; Mangin-Thro, Lucile; Karppinen, Maarit; Ward, Simon; Normand, Bruce; Rønnow, Henrik M.

Document Version
Publisher's PDF, also known as Version of record

[Link to publication on Research at Birmingham portal](#)

Randomness and frustration in a $S = \frac{1}{2}$ square-lattice Heisenberg antiferromagnet

Ellen Fogh [●],[1,*] Otto Mustonen [●],[2,3] Peter Babkevich,[1] Vamshi M. Katukuri [●],[4] Helen C. Walker [●],[5] Lucile Mangin-Thro,[6] Maarit Karppinen [●],[7] Simon Ward [●],[8] Bruce Normand,[9,1] and Henrik M. Rønnow[1]

[1]*Laboratory for Quantum Magnetism, Institute of Physics, École Polytechnique Fédérale de Lausanne (EPFL), CH-1015 Lausanne, Switzerland*
[2]*Department of Materials Science and Engineering, University of Sheffield, Mappin Street, Sheffield S1 3JD, United Kingdom*
[3]*School of Chemistry, University of Birmingham, Edgbaston, Birmingham B15 2TT, United Kingdom*
[4]*Max Planck Institute for Solid State Research, Heisenbergstrasse 1, D-70569 Stuttgart, Germany*
[5]*ISIS Neutron and Muon Source, Rutherford Appleton Laboratory, Chilton, Didcot OX11 OQX, United Kingdom*
[6]*Institute Laue Langevin, 71 Avenue des Martyrs, CS 20156, F-38042 Grenoble Cedex 9, France*
[7]*Department of Chemistry and Materials Science, Aalto University, FI-00076 Espoo, Finland*
[8]*European Spallation Source ERIC, P.O. Box 176, SE-221 00 Lund, Sweden*
[9]*Paul Scherrer Institute, CH-5232 Villigen-PSI, Switzerland*

We explore the interplay between randomness and magnetic frustration in the series of $S = \frac{1}{2}$ Heisenberg square-lattice compounds $Sr_2CuTe_{1-x}W_xO_6$. Substituting W for Te alters the magnetic interactions dramatically, from strongly nearest-neighbor to next-nearest-neighbor antiferromagnetic coupling. We perform neutron scattering measurements to probe the magnetic ground state and excitations over a range of x. We propose a bond-disorder model that reproduces ground states with only short-ranged spin correlations in the mixed compounds. The calculated neutron diffraction patterns and powder spectra agree well with the measured data and allow detailed predictions for future measurements. We conclude that quenched randomness plays the major role in defining the physics of $Sr_2CuTe_{1-x}W_xO_6$ with frustration being less significant.

I. INTRODUCTION

The Heisenberg $S = \frac{1}{2}$ square lattice with competing antiferromagnetic (AFM) nearest- and next-nearest-neighbor interactions, J_1 on the sides and J_2 on the diagonals of each square, presents a prototypical frustrated magnetic system [1,2]. As Fig. 1(a) represents, when J_1 dominates the ground state is Néel AFM order, whereas dominant J_2 gives a columnar AFM state, and a quantum spin liquid (QSL) has been proposed [3–5] within the nonordered parameter regime ($0.4 \lesssim J_2/J_1 \lesssim 0.6$) between the two AFM phases. Despite several decades of intense study, there remains no consensus over the exact nature of the QSL and the model continues to provide a focal point for QSL research.

Until recently, most such research in both experiment and theory was focused on homogenous systems, where all magnetic sites are equal. However, many real materials display intrinsic inhomogeneity, as a result of impurities or (counter)ion substitution, that results in site or bond disorder. This is known as quenched randomness, and the loss of translational symmetry it entails makes the system challenging to study theoretically. However, quenched randomness in quantum magnets can lead to specific ground states with no long-ranged order, including the Bose glass [6–11], the Mott glass [11–14], the random-singlet state [15–20], and the valence-bond glass [21–23]. These phases of matter are closely related to certain types of QSL and thus raise the question of whether randomness in a frustrated system can produce qualitatively different types of quantum coherence, as opposed to only destroying such coherence.

Here we investigate the magnetically disordered states found in the series of compounds $Sr_2CuTe_{1-x}W_xO_6$. At first sight this system seems well suited for exploring the phase diagram of the J_1-J_2 Heisenberg square lattice, because the two parent compounds, Sr_2CuTeO_6 and Sr_2CuWO_6, are respectively good J_1 and J_2 systems, displaying Néel and columnar AFM order. However, our diffuse polarized neutron diffraction and inelastic neutron scattering (INS) measurements, combined with insight from mean-field and linear spin-wave calculations, show that the $Sr_2CuTe_{1-x}W_xO_6$ family represents an altogether different but no less interesting problem. We demonstrate that the random-bond model arising from Te-W site disorder leads to a ground state of partially frozen moments in alternating patches of Néel and columnar correlations. The patch sizes depend on x, reaching a minimum of order 10 magnetic sites for $x = 0.4$. Our calculations reproduce well the experimentally observed ground and excited states, showing that disorder is more important than frustration in determining the physics of $Sr_2CuTe_{1-x}W_xO_6$.

II. MATERIALS

The isostructural materials $Sr_2CuB''O_6$ ($B'' =$ Te, W, Mo) are layered antiferromagnets in which the network of Cu^{2+} ions is well described by the J_1-J_2 square-lattice model.
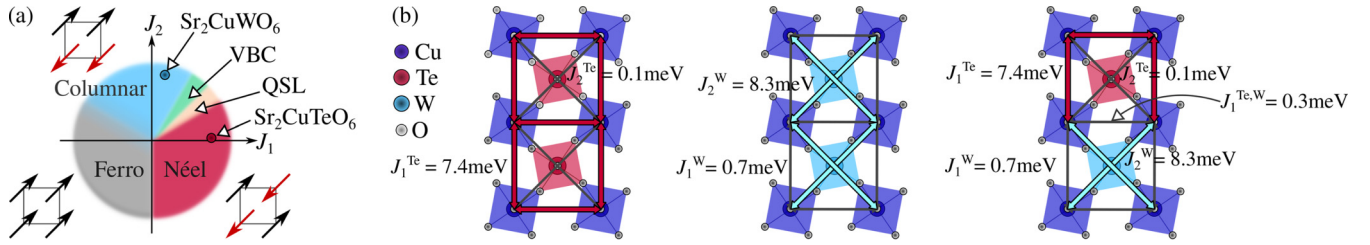
*ellen.fogh@epfl.ch

FIG. 1. The Heisenberg square lattice and $Sr_2CuTe_{1-x}W_xO_6$. (a) Phase diagram of the J_1-J_2 square-lattice Heisenberg model, showing the ferromagnetic, columnar, and Néel AFM states, as well as the frustrated parameter regimes of QSL and valence-bond crystal (VBC) behavior. (b) Magnetic interactions in $Sr_2CuTe_{1-x}W_xO_6$, represented for the three cases where the counterions in each square are both Te, both W, or one of each. The J_1 and J_2 parameters are those obtained by quantum chemistry calculations [24]; we note that the nearest-neighbor interaction is always small in the presence of W.

Neutron scattering measurements on large powder samples of the pure Te and W members of the family have shown that the ground state and spin dynamics of Sr_2CuTeO_6 are dominated by the J_1 term [25,26], whereas in Sr_2CuWO_6 they are dominated by J_2 [27,28]. The fact that Te^{6+} and W^{6+} have almost identical ionic radii [29] gives every reason to expect that mixed compounds in the series between these two end members might realize ideal random solid solutions interpolating between the J_1 and J_2 limits. X-ray diffraction studies across the doping series [30] have established that the chemical structure of the mixed systems is indeed a true solid solution for all x, and detailed characterization of the magnetic response by muon spin-rotation (μSR), specific-heat, magnetic susceptibility, and NMR measurements on $Sr_2CuTe_{0.5}W_{0.5}O_6$ [23,30,31] indicate no magnetic order above 19 mK over a wide range of doping, $0.1 \leqslant x \leqslant 0.6$, which is clearly different from a two-phase system of the end members.

In the quest to understand the dramatic difference between Sr_2CuTeO_6 and Sr_2CuWO_6, *ab initio* quantum chemistry calculations [24] have demonstrated how the Cu-Cu superexchange paths change completely due to the orbital hybridization of O $2p$ with Te^{6+} (empty $5p$) or W^{6+} (empty $5d$) [29]. The magnetic interaction parameters predicted by this analysis are shown in Fig. 1(b), and they afford the key insight that shapes both the physics of $Sr_2CuTe_{0.5}W_{0.5}O_6$ and the applicability of our spin-wave methodology, namely that all the competing bonds are very weak and hence strong local frustration is avoided. Because the substitution of a nonmagnetic ion switches the dominant Cu-Cu interaction so cleanly, while leaving the crystal structure basically unaltered, the random Te-W distribution leads to a bond-disorder problem with bimodal distributions of J_1 and J_2. Among other things, the concept of controlling a uniform J_2/J_1 ratio to obtain a QSL by substitution is not valid. Nevertheless, one may still anticipate randomness-induced magnetic disorder, as suggested by magnetic measurements on samples spanning the doping range $0.1 \leqslant x \leqslant 0.6$, [23,30,31], and recent studies have stressed the very rapid destruction of Néel order at small x [32,33] (but not at high x [32]). These results have been interpreted theoretically in terms of a random-singlet state [18,32] and of a valence-bond glass [23]. However, INS measurements show dispersive excitations similar to spin waves [24,34] and a partial freezing of random moments has been reported both at $x = 0.5$ below 1.7 K [34] and at $x = 0.05$ below 0.5 K [33]. These somewhat contradictory findings leave the

true nature of the magnetic ground state in $Sr_2CuTe_{1-x}W_xO_6$ undetermined.

III. MAGNETIC GROUND STATE

The instantaneous spin structure factor, $S(\mathbf{Q}) = \sum_j e^{i\mathbf{Q}\cdot\mathbf{r}_j} \langle \mathbf{S}_0 \cdot \mathbf{S}_j \rangle$, can be probed by diffuse polarized neutron diffraction. Here, $\mathbf{Q}$ is the momentum transfer and $\mathbf{S}_j$ the spin operator at lattice site $\mathbf{r}_j$. We collected diffraction patterns on the D7 diffractometer at the Institut Laue Langevin (ILL) using powder samples of 10–15 g of the $x = 0.2$ and $x = 0.5$ materials in Al cans at $T = 1.5$ K. The experimental wavelength of 4.8 Å corresponds to 3.55 meV, and thus captures fluctuations in the lowest 20% of the full bandwidth [26,28] by energy, which nevertheless constitute the vast majority of fluctuations by spectral weight (as we will show by INS). Thus our measurements observe the quasielastic response, or slowly fluctuating part of $S(\mathbf{Q})$. The magnetic contribution to the scattering extracted by polarization analysis [35] is shown in Fig. 2 and indicates a disordered state whose peak scattering intensity moves from 0.8 Å^{-1} for $x = 0.2$ to 0.6 Å^{-1} for $x = 0.5$, the former lying close to the magnetic Bragg peak (0.5,0.5) of Néel order and the latter to (0.5,0) of columnar order.

To interpret the diffraction data, the interaction parameters shown in Fig. 1(b) motivate a ground state for the $Sr_2CuTe_{1-x}W_xO_6$ system whose essential behavior is captured by considering only the strongest bonds, i.e., J_1^{Te} and J_2^{W}. As Fig. 3(a) makes clear, the way that the introduction of W eliminates so many J_1 bonds leads to a somewhat dilute interaction network, and in particular we observe that direct J_1-J_2 frustration, in the form of J_1-J_1-J_2 triangles, is absent in this limit. Although the physics of the ground and excited states in the random $Sr_2CuTe_{1-x}W_xO_6$ system can be understood directly from Fig. 3(a), we restore the weaker couplings in our quantitative modeling of both. For this we substitute the calculated interaction parameters [24] shown in Fig. 1(b) by the rather similar values extracted from spin-wave fits to the INS spectra of Sr_2CuTeO_6 [26] and Sr_2CuWO_6 [28], which are $J_1^{Te} = 7.6$ meV, $J_2^{Te} = 0.6$ meV, $J_1^{W} = 1.0$ meV, and $J_2^{W} = 8.5$ meV, while the undetermined coupling $J_1^{Te,W}$ is set to zero.

The spin configuration corresponding to the random-bond network for $x = 0.4$ in Fig. 3(a) is illustrated in Fig. 3(b). We calculate these configurations by updating all sites in a
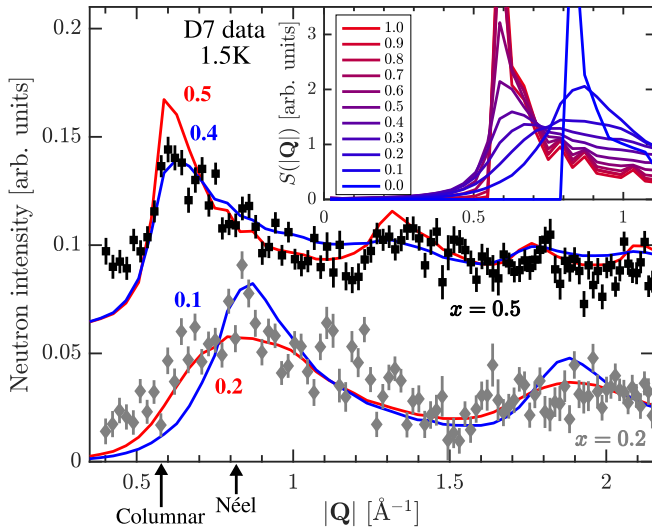
FIG. 2. Polarized neutron diffraction. Intensities measured for powder samples of $Sr_2CuTe_{1-x}W_xO_6$ with $x = 0.2$ (gray diamonds) and $x = 0.5$ (black squares). Data for $x = 0.5$ are translated upwards by 0.06 arbitrary units (arb. units) for clarity. The inset shows intensities calculated using the random-bond model of Fig. 1(b); four of these curves are scaled and superimposed on the data in the main panel.

random sequence, orienting spin i to minimize its energy, $E_i = \sum_j J_{ij}\mathbf{S}_i \cdot \mathbf{S}_j = \mathbf{S}_i \cdot \mathbf{m}_i$, in the local classical mean field, $\mathbf{m}_i = \langle J_{ij}\mathbf{S}_j \rangle$, due to all neighboring spins j. We repeat this procedure until the sum of differences in total energy from the previous 100 updates is below 10^{-9} meV for a system of 50×50 sites. The spin magnitude is fixed to $\langle S \rangle = 1/2$ and the calculation is performed for ten different random initial configurations at each value of x. We stress that all the spin configurations we obtain for $0 < x < 1$ are noncoplanar as a result of the randomness and the remaining frustration [marked in gray in Fig. 3(a)].

Averaged diffraction patterns derived from such spin structures are shown in Fig. 3(c). We find from the peaks at (0.5,0) and equivalent positions that columnar ordering predominates for $x \gtrsim 0.5$. By contrast, the (0.5,0.5) peak shows that long-ranged Néel order is destroyed even at $x \approx 0.1$ [30,32]. At intermediate x, only short-range magnetic correlations are present and the scattering is not isotropic, but forms instead a rounded, crosslike pattern in $S(\mathbf{Q})$. This indicates the presence of coexisting regions of very short-ranged Néel and columnar order, a real-space picture confirmed in Fig. 3(b). The sizes of these "patches" depend on x, and are of order 10 magnetic sites for $x = 0.4$.

The powder averages of the diffraction patterns in Fig. 3(c) are shown in the inset of Fig. 2. Because the spins in our mean-field calculations are static, the comparison with the slowly fluctuating part of $S(\mathbf{Q})$, as probed by our D7 measurements, is fully justified. While it is clear that our model is entirely consistent with the observed diffuse diffraction signal, we cannot exclude other models on the basis of Fig. 2 alone. One prominent example is the response of sizable magnetic domains of Néel and columnar order, which would give only broadened peaks at the Bragg positions in Fig. 3(c), but on powder averaging would be difficult to distinguish
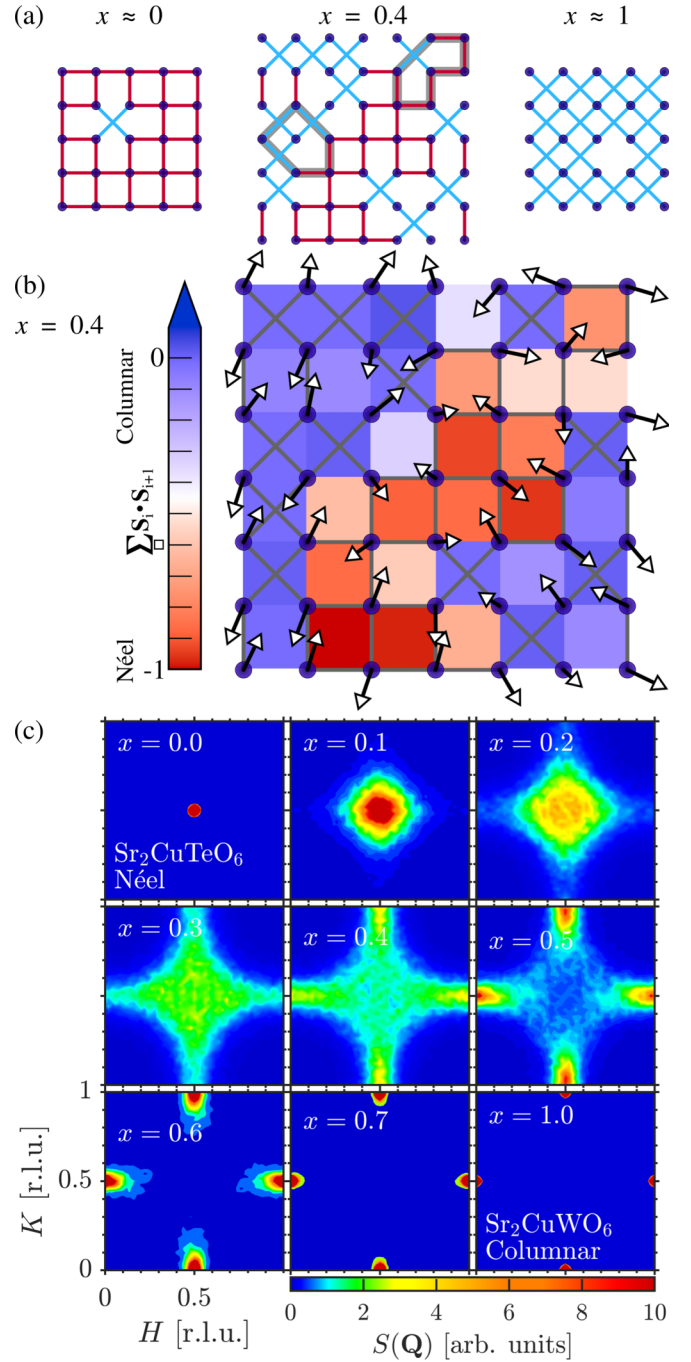
FIG. 3. Ground-state spin configurations. (a) Examples of random-bond networks for $Sr_2CuTe_{1-x}W_xO_6$ with $x \approx 0$, $x = 0.4$, and $x \approx 1$; weak interactions are omitted for clarity. Thick gray lines at $x = 0.4$ indicate two representative geometrically frustrated paths, with five bonds being the shortest possible. (b) Spin configuration for $x = 0.4$, matching the bond network in (a). The color code quantifies the correlations around each square, $\sum_\square \mathbf{S}_i \cdot \mathbf{S}_{i+1}$ ($i = \{1, 2, 3, 4\}$ labeling the four sites), which vary from Néel (red) to columnar (blue) character. Because the spins are of fixed size but rotate in three dimensions, shorter arrows indicate an out-of-plane component. (c) Calculated structure factor $S(\mathbf{Q})$ showing the evolution from Néel to columnar order. Only for $x = 0$ and 1 are the peaks very sharp, as expected for long-range order.
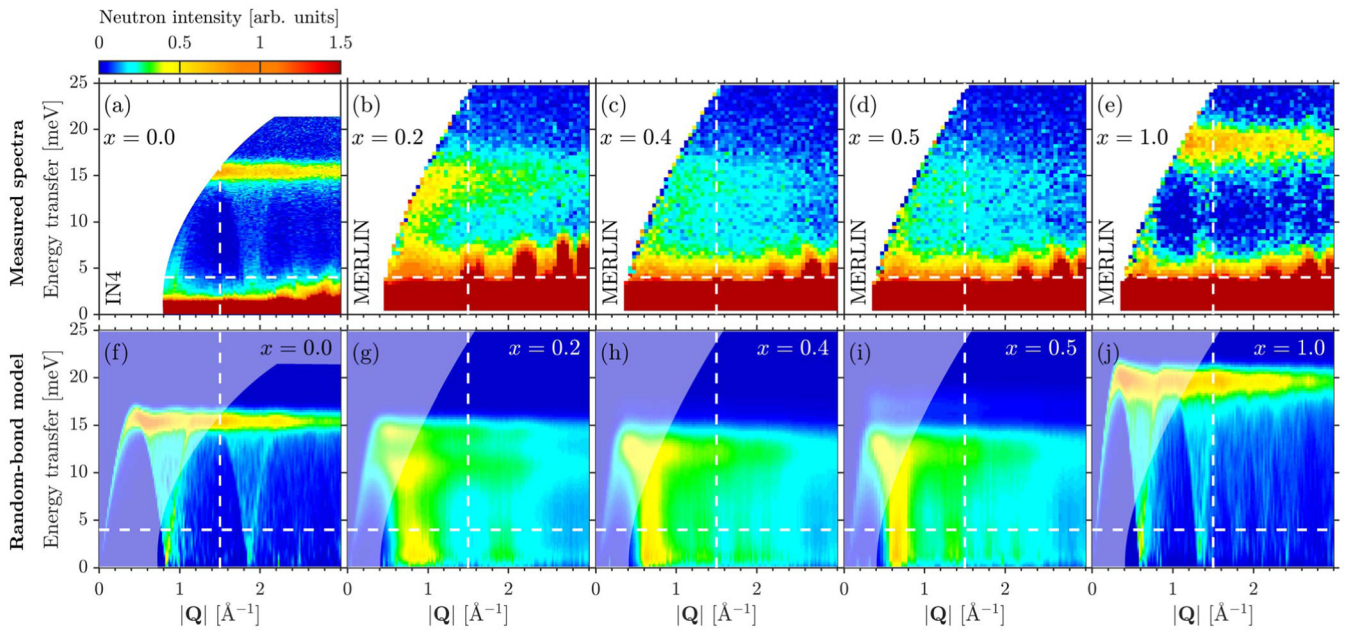
FIG. 4. Magnetic excitations in $Sr_2CuTe_{1-x}W_xO_6$. (a)–(e) Powder INS spectra for samples with $x = 0, 0.2, 0.4, 0.5,$ and 1, normalized to the nuclear Bragg peak for comparison between different x values. (f)–(j) Spectra calculated using the random-bond model. The magnetic form factor for Cu^{2+} was estimated following Ref. [36] and an energy broadening ($dE = 1.2$ meV for $x = 0$ and 1.8 meV for $x > 0$) was convolved with each calculated spectrum to approximate the instrumental resolution. Regions of $|\mathbf{Q}|$ not covered in experiment are dimmed in the modeled spectra. The dashed lines mark the constant $|\mathbf{Q}|$ and energy values analyzed in Fig. 5.

from our measurements. However, such a superposition could not explain the complete lack of magnetic order observed by μSR and INS for $0.05 \leqslant x \leqslant 0.6$, and next we turn to our measurements of the spin dynamics to obtain further information.

IV. SPIN DYNAMICS

Our INS experiments were performed at the time-of-flight spectrometer MERLIN [37] at the ISIS Neutron and Muon Source, using 10-g powder samples of the $x = 0.2, 0.4, 0.5,$ and 1 materials in Al cans, with an incoming neutron energy of 45 meV and at a temperature of 5 K. In the spectra shown in Figs. 4(a)–4(e), a thermally adjusted background factor (recorded above 100 K) was subtracted to remove the phonon contribution at larger $|\mathbf{Q}|$. The $x = 0$ data are those of Ref. [26]. The pure compounds Sr_2CuTeO_6 and Sr_2CuWO_6 show spin waves dispersing respectively from the zone centers of Néel and columnar order. Bands of strong scattering found around 16 meV for $x = 0$ and 18 meV for $x = 1$ correspond to van Hove singularities at the zone boundaries. Although the spectra of the mixed $Sr_2CuTe_{1-x}W_xO_6$ compounds show strong broadening in momentum and energy transfer, both the low-energy dispersive features and the van Hove band remain present.

The success of the random-bond model in reproducing the ground states of the mixed systems (Fig. 2) suggests its utility for analyzing their excitations. Despite having no long-range order, the mean-field states have frozen moments and thus we can compute powder-averaged INS spectra by using linear spin-wave theory, as implemented in the software package SPINW [38]. We define supercells of 10×10 sites with random-bond distributions of the type shown in Fig. 3(b)

and periodic boundary conditions; for each value of x, we average the results from five different random configurations. For maximally quantitative modeling, we apply the series-expansion correction factor $Z_c = 1.18$ [39] to our calculated energies. The resulting spectra, shown in Figs. 4(f)–4(j), make clear that the random-bond model captures all the primary features of the measured spectra. Spin-wave-type modes, with substantial broadening in $|\mathbf{Q}|$ and energy, remain centered at 0.8 Å^{-1} for $x = 0.2$, transitioning to 0.6 Å^{-1} for $x = 0.5$, while the calculated bandwidth reduction is in quantitative agreement with the data.

For further comparison, in Fig. 5(a) we show a constant-$|\mathbf{Q}|$ cut through the spectrum at $|\mathbf{Q}| = 1.5$ Å^{-1}, where strong scattering is observed around 16 meV for Sr_2CuTeO_6 and 18 meV for Sr_2CuWO_6. For $x = 0.2, 0.4,$ and 0.5, these van Hove peaks become a broad feature around 12–15 meV that is reproduced accurately by our modeling, as shown in Fig. 5(b). The increased scattering observed below 10 meV is the tail of the broadened elastic line, which we do not model. Similarly, a constant-energy cut at 4 meV, examined as a function of $|\mathbf{Q}|$ in Figs. 5(c) and 5(d), captures the excitations dispersing upwards from the magnetic zone centers. For Sr_2CuTeO_6 and Sr_2CuWO_6, the first spin-wave branches emerge respectively from $|\mathbf{Q}| = 0.8$ and 0.6 Å^{-1}, while the excitations from the next Brillouin zone are found at $|\mathbf{Q}| = 1.8$ and 1.3 Å^{-1}. As Te is replaced by W, these low-energy excitations change rapidly to resemble those of Sr_2CuWO_6, such that the spectra of the $x = 0.4$ and 0.5 compounds show the fingerprints mostly of the $x = 1$ system [both the (0.5,0) and (0.5,1.5) features strengthening from $x = 0.4$ to 0.5]. We stress that our modeling procedure has no free parameters, but clearly reproduces all the essential features of the $Sr_2CuTe_{1-x}W_xO_6$ system at a semiquantitative level.
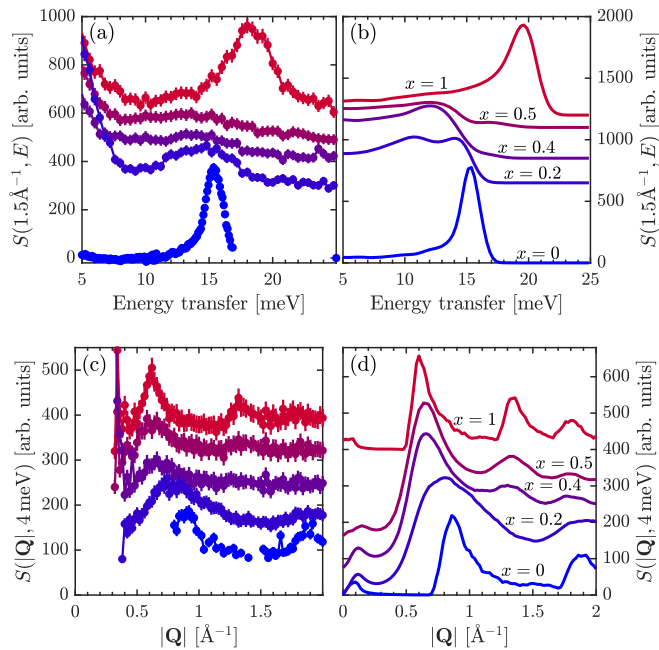
FIG. 5. Dynamical structure factor. Measured (left) and calculated (right panels) $S(|\mathbf{Q}|, E)$ at constant $|\mathbf{Q}| = 1.5$ Å^{-1} (top) and constant $E = 4$ meV (bottom panels). The respective integration widths are $\Delta|\mathbf{Q}| = 0.2$ Å^{-1} and $\Delta E = 2$ meV. The curves are offset along the y axis for clarity.

V. DISCUSSION AND CONCLUSIONS

Thus we have shown that the $Sr_2CuTe_{1-x}W_xO_6$ series realizes not highly frustrated magnetism but a random-bond model whose ground state at intermediate x is a partially frozen disorder. This situation is a consequence of the strong suppression of J_1 bonds as soon as one neighboring Te site is substituted by W [24]: Fig. 3(a) illustrates that, if one neglects the 10% effect of the subdominant bonds, then no triangles are created and the shortest frustrated paths consist of five bonds, which furthermore are rather sparse within the bonding network. With such moderate geometric frustration, short-range order forms over patches considerably larger than the individual squares, as shown in Fig. 3(b). This partial frustration release explains why a semiclassical spin-wave and mean-field treatment captures the leading behavior of the maximally quantum mechanical $S = \frac{1}{2}$ spin system reasonably well, even when more complex combinations of the different bonds ($J_1^{Te}, J_2^{Te}, J_1^W, J_2^W$) are used. Here, we stress that quantum-fluctuation corrections to our analysis can act to reduce some local moments to zero, and future neutron diffraction studies could probe this site-dependent effect. Nevertheless, our experimental data and calculations suggest that the ground state is a percolating network of frozen, randomly oriented average moments, within which some sites and patches may be fully fluctuating.

The possible existence of a weak frozen-moment phase is emerging as a key question in the understanding of bond randomness in $S = \frac{1}{2}$ quantum magnets. Although early μSR measurements indicating no magnetic order down to sub-K temperatures for $Sr_2CuTe_{1-x}W_xO_6$ with $0.1 \leqslant x \leqslant 0.6$, together with a T-linear specific heat, were suggested initially as

evidence for a QSL state [30,31], further μSR investigations at very small x are being interpreted [32,33] as evidence for the onset of a dominant random-singlet phase. The distinction between the random-singlet [17–19] and valence-bond-glass phases [23] is that all singlets in the latter state have finite gaps, whereas in the former they form a continuum of values to the gapless limit. However, INS data indicating a transition from liquid to weakly frozen behavior below 1.7 K for $x = 0.5$ [34] and the μSR observation of a frozen component below 0.5 K at $x = 0.05$ [33] raise the question of whether a random frozen spin network can persist as an intermediate regime as long-range order is destroyed by bond randomness.

Our results provide a qualitative basis on which to interpret these findings. Although both the diffuse diffraction pattern and the spin-wave-type excitations we observe are consistent with a random network, the finite momentum resolution in our experiment and the lack of quantum corrections in our model prevent an unambiguous conclusion. The fact that reports of a finite frozen moment are restricted to the low [33] and high [34] ends of the substitution range for the suppression of long-range order suggests that x may be an important factor in controlling the crossover to an entirely disordered (fluctuating, moment-free) ground state. The other key factor is likely to be the residual frustration, where our results suggest that $Sr_2CuTe_{1-x}W_xO_6$ may lack the degree of frustration required to realize an unconventional all-singlet disordered state, but a system with stronger local frustration could indeed do so. On this note we stress that the $Sr_2CuTe_{1-x}W_xO_6$ family remains an excellent framework for studying the interplay between randomness and frustration in $S = \frac{1}{2}$ quantum magnets. The bond randomness of $Sr_2CuTe_{1-x}W_xO_6$ also arises in systems including $Ba_2Cu(Te, W)O_6$ [40,41] and $Cr_2(Te, W)O_6$ [42,43], and we expect these compounds to allow a further investigation of exotic magnetic states at the nexus of disorder and frustration.

In summary, we have presented neutron diffraction data and INS spectra for the J_1-J_2 square-lattice system $Sr_2CuTe_{1-x}W_xO_6$ with $0 \leqslant x \leqslant 1$ and we have introduced a matching random-bond model based on *ab initio* calculations. The model diffraction pattern in the magnetically disordered region ($0.1 < x < 0.5$) has a crosslike form that is fully consistent with our diffuse polarized neutron diffraction measurements. The ground state consists of small patches of predominantly nearest- or next-nearest-neighbor correlated spins dictated by the nonmagnetic dopant sites. Powder spectra obtained from the random-bond model reproduce the dispersive excitations and suppressed band maximum observed in our INS experiments. These findings show that it is the bond randomness in $Sr_2CuTe_{1-x}W_xO_6$, rather than the residual frustration, that drives the physics of the system.

[1] P. Chandra and B. Doucot, Possible spin-liquid state at large S for the frustrated square Heisenberg lattice, Phys. Rev. B **38**, 9335(R) (1988).

[2] R. Darradi, O. Derzhko, R. Zinke, J. Schulenburg, S. E. Krüger, and J. Richter, Ground state phases of the spin-1/2 J_1-J_2 Heisenberg antiferromagnet on the square lattice: A high-order coupled cluster treatment, Phys. Rev. B **78**, 214415 (2008).

[3] S. Morita, R. Kaneko, and M. Imada, Quantum spin liquid in spin 1/2 J_1-J_2 Heisenberg model on square lattice: Many-variable variational Monte Carlo study combined with quantum-number projections, J. Phys. Soc. Jpn. **84**, 024720 (2015).

[4] S.-S. Gong, W. Zhu, D. N. Sheng, O. I. Motrunich, and M. P. A. Fisher, Plaquette Ordered Phase and Quantum Phase Diagram in the Spin-1/2 J_1-J_2 Square Heisenberg Model, Phys. Rev. Lett. **113**, 027201 (2014).

[5] L. Wang and A. W. Sandvik, Critical Level Crossings and Gapless Spin Liquid in the Square-Lattice Spin-1/2 J_1-J_2 Heisenberg Antiferromagnet, Phys. Rev. Lett. **121**, 107202 (2018).

[6] M. P. A. Fisher, P. B. Weichman, G. Grinstein, and D. S. Fisher, Boson localization and the superfluid-insulator transition, Phys. Rev. B **40**, 546 (1989).

[7] N. Prokof'ev and B. Svistunov, Superfluid-Insulator Transitions in Commensurate Disordered Bosonic Systems: Large-Scale Worm Algorithm Simulations, Phys. Rev. Lett. **92**, 015703 (2004).

[8] E. Altman, Y. Kafri, A. Polkovnikov, and G. Refael, Phase Transition in a System of One-Dimensional Bosons with Strong Disorder, Phys. Rev. Lett. **93**, 150402 (2004).

[9] O. Nohadani, S. Wessel, and S. Haas, Bose-Glass Phases in Disordered Quantum Magnets, Phys. Rev. Lett. **95**, 227201 (2005).

[10] H. Manaka, A. V. Kolomiets, and T. Goto, Disordered States in IPA-Cu(Cl$_x$Br$_{1-x}$)$_3$ Induced by Bond Randomness, Phys. Rev. Lett. **101**, 077204 (2008).

[11] R. Yu, L. Yin, N. S. Sullivan, J. S. Xia, C. Huan, A. Paduan-Filho, N. F. Oliveira Jr., S. Haas, A. Steppke, C. F. Miclea, F. Weickert, R. Movshovich, E.-D. Mun, V. S. Zapf, and T. Roscilde, Bose glass and Mott glass of quasiparticles in a doped quantum magnet, Nature (London) **489**, 379 (2012).

[12] E. Orignac, T. Giamarchi, and P. L. Doussal, Possible New Phase of Commensurate Insulators with Disorder: The Mott Glass, Phys. Rev. Lett. **83**, 2378 (1999).

[13] E. Altman, Y. Kafri, A. Polkovnikov, and G. Refael, Insulating Phases and Superfluid-Insulator Transition of Disordered Boson Chains, Phys. Rev. Lett. **100**, 170402 (2008).

[14] L. Savary and L. Balents, Disorder-Induced Quantum Spin Liquid in Spin Ice Pyrochlores, Phys. Rev. Lett. **118**, 087203 (2017).

[15] R. N. Bhatt and P. A. Lee, Scaling Studies of Highly Disordered Spin-1/2 Antiferromagnetic Systems, Phys. Rev. Lett. **48**, 344 (1982).

[16] D. S. Fisher, Random antiferromagnetic quantum spin chains, Phys. Rev. B **50**, 3799 (1994).

[17] L. Liu, H. Shao, Y.-C. Lin, W. Guo, and A. W. Sandvik, Random-Singlet Phase in Disordered Two-Dimensional Quantum Magnets, Phys. Rev. X **8**, 041040 (2018).

[18] K. Uematsu and H. Kawamura, Randomness-induced quantum spin liquid behavior in the $s = \frac{1}{2}$ random J_1-J_2 Heisenberg antiferromagnet on the square lattice, Phys. Rev. B **98**, 134427 (2018).

[19] H.-D. Ren, T.-Y. Xiong, H.-Q. Wu, D. N. Sheng, and S.-S. Gong, Characterizing random-singlet state in two-dimensional frustrated quantum magnets and implications for the double perovskite Sr$_2$CuTe$_{1-x}$W$_x$O$_6$, arXiv:2004.02128.

[20] S.-H. Baek, H. W. Yeo, S.-H. Do, K.-Y. Choi, L. Janssen, M. Vojta, and B. Büchner, Observation of a random singlet state in a diluted Kitaev honeycomb material, Phys. Rev. B **102**, 094407 (2020).

[21] M. Tarzia and G. Biroli, The valence bond glass phase, Europhys. Lett. **82**, 67008 (2008).

[22] R. R. P. Singh, Valence Bond Glass Phase in Dilute Kagome Antiferromagnets, Phys. Rev. Lett. **104**, 177203 (2010).

[23] M. Watanabe, N. Kurita, H. Tanaka, W. Ueno, K. Matsui, and T. Goto, Valence-bond-glass state with a singlet gap in the spin-$\frac{1}{2}$ square-lattice random J_1-J_2 Heisenberg antiferromagnet Sr$_2$CuTe$_{1-x}$W$_x$O$_6$, Phys. Rev. B **98**, 054422 (2018).

[24] V. M. Katukuri, P. Babkevich, O. Mustonen, H. C. Walker, B. Fåk, S. Vasala, M. Karppinen, H. M. Rønnow, and O. V. Yazyev, Exchange Interactions Mediated by Non-Magnetic Cations in Double Perovskites, Phys. Rev. Lett. **124**, 077202 (2020).

[25] T. Koga, N. Kurita, M. Avdeev, S. Danilkin, T. J. Sato, and H. Tanaka, Magnetic structure of the $S = \frac{1}{2}$ quasi-two-dimensional square-lattice Heisenberg antiferromagnet, Phys. Rev. B **93**, 054426 (2016).

[26] P. Babkevich, V. M. Katukuri, B. Fåk, S. Rols, T. Fennell, D. Pajić, H. Tanaka, T. Pardini, R. R. P. Singh, A. Mitrushchenkov, O. V. Yazyev, and H. M. Rønnow, Magnetic Excitations and Electronic Interactions in Sr$_2$CuTeO$_6$: A Spin-1/2 Square Lattice Heisenberg Antiferromagnet, Phys. Rev. Lett. **117**, 237203 (2016).

[27] S. Vasala, M. Avdeev, S. Danilkin, O. Chmaissem, and M. Karppinen, Magnetic structure of Sr$_2$CuWO$_6$, J. Phys.: Condens. Matter **26**, 496001 (2014).

[28] H. C. Walker, O. Mustonen, S. Vasala, D. J. Voneshen, M. D. Le, D. T. Adroja, and M. Karppinen, Spin wave excitations in the tetragonal double perovskite Sr$_2$CuWO$_6$, Phys. Rev. B **94**, 064411 (2016).

[29] R. D. Shannon, Revised effective ionic radii and systematic studies of interatomic distances in halides and chalcogenides, Acta Crystallogr., Sect. A **32**, 751 (1976).

[30] O. Mustonen, S. Vasala, K. P. Schmidt, E. Sadrollahi, H. C. Walker, I. Terasaki, F. J. Litterst, E. Baggio-Saitovitch, and M. Karppinen, Tuning the $S = 1/2$ square-lattice antiferromagnet

$Sr_2Cu(Te_{1-x}W_x)O_6$ from Néel order to quantum disorder to columnar order, Phys. Rev. B **98**, 064411 (2018).

[31] O. Mustonen, S. Vasala, E. Sadrollahi, K. P. Schmidt, C. Baines, H. C. Walker, F. J. Litterst, E. Baggio-Saitovitch, and M. Karppinen, Spin-liquid-like state in a spin-1/2 square-lattice antiferromagnet perovskite induced by d^{10}-d^0 cation mixing, Nat. Commun. **9**, 1085 (2018).

[32] W. Hong, L. Liu, C. Liu, X. Ma, A. Koda, X. Li, J. Song, W. Yang, J. Yang, P. Cheng, H. Zhang, W. Bao, X. Ma, D. Chen, K. Sun, W. Guo, H. Luo, A. W. Sandvik, and S. Li, Extreme Suppression of Antiferromagnetic Order and Critical Scaling in a Two-Dimensional Random Quantum Magnet, Phys. Rev. Lett. **126**, 037201 (2021).

[33] S. Yoon, W. Lee, S. Lee, J. Park, C. H. Lee, Y. S. Choi, S.-H. Do, W.-J. Choi, W.-T. Chen, F. Chou, D. I. Gorbunov, Y. Oshima, A. Ali, Y. Singh, A. Berlie, I. Watanabe, and K.-Y. Choi, Quantum disordered state in the J_1-J_2 square lattice antiferromagnet $Sr_2Cu(Te_{0.95}W_{0.05})O_6$, Phys. Rev. Materials **5**, 014411 (2021).

[34] X. Hu, D. M. Pajerowski, D. Zhang, A. A. Podlesnyak, Y. Qiu, Q. Huang, H. Zhou, I. Klich, A. I. Kolesnikov, M. B. Stone, and S.-H. Lee, Freezing of a Disorder Induced Spin Liquid with Strong Quantum Fluctuations, Phys. Rev. Lett. **127**, 017201 (2021).

[35] G. Ehlers, J. R. Stewart, A. R. Wildes, P. P. Deen, and K. H. Andersen, Generalization of the classical *xyz*-polarization analysis technique to out-of-plane and inelastic scattering, Rev. Sci. Instrum. **84**, 093901 (2013).

[36] *International Tables for Crystallography*, edited by E. Prince (Kluwer Academic, Dordrecht, 2004), Chaps. 4.4.5 and 6.1.2.

[37] R. I. Bewley, T. Guidi, and S. Bennington, MERLIN: A high count rate chopper spectrometer at ISIS, Notiziario Neutroni e Luce di Sincrotrone **14**, 22 (2009).

[38] S. Toth and B. Lake, Linear spin wave theory for single-Q incommensurate magnetic structures, J. Phys.: Condens. Matter **27**, 166002 (2015).

[39] R. R. P. Singh, Thermodynamic parameters of the $T = 0$, spin-1/2 square-lattice Heisenberg antiferromagnet, Phys. Rev. B **39**, 9760 (1989).

[40] O. Mustonen, S. Vasala, H. Mutch, C. I. Thomas, G. B. G. Stenning, E. Baggio-Saitovitch, E. J. Cussen, and M. Karppinen, Magnetic interactions in the $S = 1/2$ square-lattice antiferromagnets Ba_2CuTeO_6 and Ba_2CuWO_6: Parent phases of a possible spin liquid, Chem. Commun. **55**, 1132 (2019).

[41] O. H. J. Mustonen, C. E. Pughe, H. C. Walker, H. M. Mutch, G. B. G. Stenning, F. C. Coomer, and E. J. Cussen, Diamagnetic d-orbitals drive magnetic structure selection in the double perovskite Ba_2MnTeO_6, Chem. Mater. **32**, 7070 (2020).

[42] M. Zhu, D. Do, C. R. D. Cruz, Z. Dun, H. D. Zhou, S. D. Mahanti, and X. Ke, Tuning the Magnetic Exchange via a Control of Orbital Hybridization in $Cr_2(Te_{1-x}W_x)O_6$, Phys. Rev. Lett. **113**, 076406 (2014).

[43] M. Zhu, D. Do, C. R. D. Cruz, Z. Dun, J.-G. Cheng, H. Goto, Y. Uwatoko, T. Zou, H. D. Zhou, S. D. Mahanti, and X. Ke, Ferromagnetic superexchange in insulating Cr_2MoO_6 by controlling orbital hybridization, Phys. Rev. B **92**, 094419 (2015).

[44] P. Babkevich, B. Fåk, S. Rols, H. M. Rønnow, and H. Tanaka, Competing interactions in low-dimensional spin system Sr_2CuTeO_6, Institut Laue-Langevin (ILL) (2015), doi:10.5291/ILL-DATA.4-01-1477.

[45] P. Babkevich, E. Fogh, T. Hansen, L. Mangin-Thro, O. Mustonen, H. M. Rønnow, and H. C. Walker, Bond disorder on a two-dimensional square lattice of the antiferromagnetic $Sr_2Cu(W,Te)O_6$, Institut Laue-Langevin (ILL) (2019), doi:10.5291/ILL-DATA.5-31-2638.

[46] H. C. Walker, O. H. Mustonen, D. T. Adroja, M. Karppinen, S. Vasala, and T. Tiittanen, INS study of double perovskite at the border between two and three dimensional magnetism, ISIS Neutron and Muon Source (2015), doi:10.5286/ISIS.E.RB1520052.

[47] M. Karppinen, O. H. Mustonen, H. C. Walker, D. T. Adroja, and S. Vasala, Inelastic neutron scattering investigation of Sr_2CuTeO_6, ISIS Neutron and Muon Source (2016), doi:10.5286/ISIS.E.RB1620093.

[48] P. Babkevich, H. C. Walker, H. M. Rønnow, and O. H. Mustonen, Exploring a potential spin-liquid candidate $Sr_2CuTe_{0.2}W_{0.8}O_6$ compound, ISIS Neutron and Muon Source (2018), doi:10.5286/ISIS.E.RB1890186-1.